Acta Crystallographica Section B
Structural Science
ISSN 0108-7681

Structures of three substituted arenesulfonamides from X-ray powder diffraction data using the differential evolution technique

Maryjane Tremayne,[a]* Colin C. Seaton[a] and Christopher Glidewell[b]

[a]School of Chemical Sciences, University of Birmingham, Edgbaston, Birmingham B15 2TT, UK, and [b]School of Chemistry, University of St Andrews, St Andrews, Fife KY16 9ST, UK

Correspondence e-mail: m.tremayne@bham.ac.uk

Received 22 April 2002
Accepted 5 July 2002

The structures of three substituted arenesulfonamides have been solved from laboratory X-ray powder diffraction data, using a new direct-space structure solution method based on a differential evolution algorithm, and refined by the Rietveld method. In 2-toluenesulfonamide, $C_7H_9NO_2S$ (I) (tetragonal $I4_1/a$, $Z = 16$), the molecules are linked by N—H···O═S hydrogen bonds into a three-dimensional framework. In 3-nitrobenzenesulfonamide, $C_6H_6N_2O_4S$ (II) (monoclinic $P2_1$, $Z = 2$), N—H···O═S hydrogen bonds produce molecular ladders, which are linked into sheets by C—H···O═S hydrogen bonds: the nitro group does not participate in the hydrogen bonding. Molecules of 4-nitrobenzenesulfonamide, $C_6H_6N_2O_4S$ (III) (monoclinic $P2_1/n$, $Z = 4$), are linked into sheets by four types of hydrogen bond, N—H···O═S, N—H···O(nitro), C—H···O═S and C—H···O(nitro), and the sheets are weakly linked by aromatic $\pi\cdots\pi$ stacking interactions.

1. Introduction

Several years ago, we reported the structure solution and refinement of a number of arenesulfonamides, using X-ray powder diffraction data collected on a conventional laboratory powder diffractometer (Lightfoot *et al.*, 1993). However, two of the examples studied at that time, 2,4,6-triisopropylbenzenesulfonamide, $(Me_2CH)_3C_6H_2SO_2NH_2$, and 2-toluenesulfonamide, $CH_3C_6H_4SO_2NH_2$ (I), could not be solved using the data and the algorithms then available. More recently, we have reported (Tremayne *et al.*, 1999) the structure of 2,4,6-triisopropylbenzenesulfonamide, which was solved and refined using synchrotron data and the Monte Carlo structure solution method (Harris *et al.*, 1994). For compound (I), the original data were indexed on a tetragonal cell, with $Z = 16$ and probable space group $I4_1/a$, but no solution was possible (Lightfoot *et al.*, 1993). Using a new direct-space structure solution technique based on differential evolution, we have now solved this structure using the original data. Here, we report the results of the solution and refinement, which show that the molecules are linked by N—H···O═S hydrogen bonds into a very elegant three-dimensional framework. We have also reanalysed the supramolecular aggregation patterns of some arenesulfonamides and arenesulfonylhydrazines for which the original structure report did not include H atoms (Lightfoot *et al.*, 1993), and we compare the supramolecular structure of compound (I) with those of four other simple arenesulfonamides and arenesulfonylhydrazines, all determined from X-ray powder diffraction data.

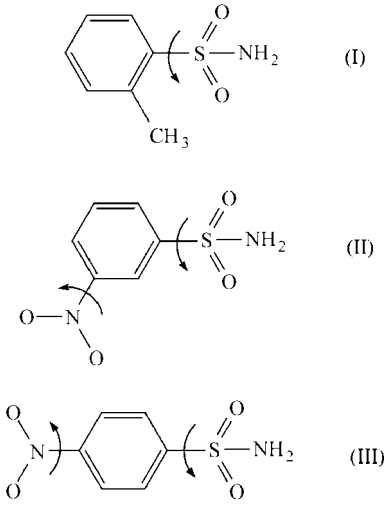

Scheme 1

In addition to the structure solution of (I), we have used this new method to determine the structures of two nitrobenzenesulfonamides, 3-nitrobenzenesulfonamide (II) and 4-nitrobenzenesulfonamide (III) ($C_6H_6N_2O_4S$), also from conventional laboratory powder data. Introduction of nitro groups into arenesulfonamides allows for competition between hard (Braga *et al.*, 1995) hydrogen bonds of types N—H···O═S and N—H···O(nitro). The dominant modes of supramolecular aggregation in sulfonamides (Vorontsova, 1966; Klug, 1968, 1970; Cotton & Stokely, 1970; Blaschette *et al.*, 1986; Brink & Mattes, 1986; Lightfoot *et al.*, 1993; Tremayne *et al.*, 1999) are by means of $C(4)$ chains and $R_2^2(8)$ rings (Bernstein *et al.*, 1995), while in simple nitroanilines N—H···O hydrogen bonds can lead to supramolecular aggregation in one, two or three dimensions (Ploug-Sørensen & Andersen, 1986; Tonogaki *et al.*, 1993; Ellena *et al.*, 1999; Cannon *et al.*, 2001; Ferguson *et al.*, 2001). Hence, the isomeric nitrobenzenesulfonamides provide a test of the competitive interplay between the two types of hard hydrogen bond, possibly augmented by the two alternative soft (Braga *et al.*, 1995) hydrogen bond types, C—H···O═S and C—H···O(nitro).

The structure determination of molecular materials from powder diffraction data is a rapidly expanding field (Harris & Tremayne, 1996; Harris *et al.*, 2001), due mostly to the recent advances in the development of direct-space methods of structure solution. These approach structure solution by the generation of trial crystal structures based on the known molecular connectivity of the material, and assessment of the fitness of each structure by comparison between the calculated diffraction pattern for each structure and the experimental data. Global optimization methods such as Monte Carlo (Harris *et al.*, 1994; Tremayne *et al.*, 1997, 1999; Tremayne & Glidewell, 2000), simulated annealing (Andreev *et al.*, 1997; Andreev & Bruce, 1998; David *et al.*, 1998; Pagola *et al.*, 2000; Shankland *et al.*, 2001; Nowell *et al.*, 2002) or genetic algorithms (Kariuki *et al.*, 1997; Harris *et al.*, 1998; Shankland *et al.*, 1998; Tedesco *et al.*, 2001; Cheung *et al.*, 2002) are then used to locate the minimum corresponding to the structure solution. In this paper, we demonstrate the application of a new global optimization technique based on differential evolution (DE) to structure solution from powder diffraction data (Seaton & Tremayne, 2002*a*). DE is an algorithm based on evolutionary principles and offers robust searching of minima (Price, 1999) while remaining a relatively simple method to implement.

As with many systems of interest in supramolecular chemistry, these sulfonamide materials are ideal for study using direct-space structure solution techniques, with the organization of molecular building blocks within the crystal structure being of greatest importance. These methods enable us to rationalize the structures of materials important in the study of intermolecular interactions, such as cocrystals (Tremayne & Glidewell, 2000) or compounds that are part of a systematic crystallographic study but do not form crystals suitable for single-crystal diffraction (Aakeröy *et al.*, 2001). Development of the DE technique has enabled us to extend our study of sulfonylamino compounds to the structure determination of a total of seven arenesulfonamides entirely from powder diffraction data. Apart from our earlier study of compound (I) (Lightfoot *et al.*, 1993) the only other crystallographic report on this material confined itself to recording the cell dimensions and space group (Burgeni *et al.*, 1929): there have been no previous reports on any of the nitrobenzenesulfonamides.

2. Differential evolution

2.1. Methodology

The direct-space approach to structure solution from powder diffraction data involves the movement of a collection of atoms, forming the structural model, around the unit cell to generate trial crystal structures that are described by a list of elements: *e.g.* the position (x, y, z) and orientation $(\theta, \varphi, \gamma)$ of a molecular model in the unit cell and the conformation of the molecule defined by variable torsion angles $(\tau_1 \ldots \tau_n)$. Each trial structure is ranked by crystallographic R_{wp} (or χ^2), and a global optimization procedure is used to explore this R_{wp} hypersurface to locate the global minimum or the best structure solution (that with lowest R_{wp}).

Sequential optimization algorithms such as Monte Carlo or simulated annealing operate on a single trial structure, whereas evolutionary algorithms such as DE or genetic algorithms maintain a population of trial structures (or members), which are mutated and recombined together over a number of generations. These evolutionary methods differ mainly in the processes used for mutation and recombination.

DE is a relatively new evolutionary algorithm that was originally developed to solve the Chebychev polynomial fitting problem (Storn & Price, 1997) and was subsequently entered into the first International Contest on Evolutionary Computation, where it was the highest placed method that did not use specialized problem information (Chisholm, 1999). For each member of the DE population, a child is created by

summation of the weighted differences of randomly selected members of the population (1):

$$\text{Trial} = \text{Parent} + K(\text{Random}_1 - \text{Parent}) + F(\text{Random}_2 - \text{Random}_3). \quad (1)$$

The term $K(\text{Random}_1 - \text{Parent})$ was introduced to overcome the limitations of the initial implementation (Storn & Price, 1997) in cases where the parameters used to define the problem are correlated. This can be considered as the recombination step and the term $F(\text{Random}_2 - \text{Random}_3)$ as the mutation. Hence, the parameters K and F can be used to adjust the level of recombination or mutation for a given run and change the search dynamic. This performs the recombination and mutation together in a single step and generates the new population in a deterministic manner by comparison of the child with its parent, where the superior of the two is added to the new population. The whole process is repeated for a fixed number of generations or until convergence to a minimum is achieved.

The use of this method of recombination along with the deterministic method of selection means that DE is a simpler method to implement than other techniques, such as genetic algorithms, in which a series of recombination and mutation steps are performed on randomly selected members of the population and the new population is probabilistically selected (Harris *et al.*, 1998). The reduced number of user-defined parameters in DE (population size N_p, maximum number of generations G_{max}, K and F) compared with other evolutionary methods also means that it is easier to understand the role that each variable plays in controlling the dynamics of the method through systematic variation. The selection method used here results in a population that retains higher diversity for longer than may be possible for other methods, and hence with slower convergence a more robust search of the hypersurface is possible. The generation of children by consideration of the difference between existing members in the population also means that the algorithm adapts to the search hypersurface as time proceeds, with the mutation term continually changing through the runtime of the program.

2.2. Implementation

The DE method utilizes a population of structures that are randomly initialized within the limits given for each element (x, y, z, θ, φ, γ, $\tau_1 \ldots \tau_n$). Each of these elements has an associated upper and lower bound, which is checked by the DE algorithm when trial structures are generated. If the value of any of these elements exceeds the corresponding bounds, it is reset to a median value between the parent and the boundary. This procedure allows the incorporation of geometrical limits (*i.e.* prior knowledge of areas of molecular conformation), while enhancing the efficiency of the search rather than disrupting the natural optimization pathways.

The parameters used to control the DE calculation are determined by the complexity of the structure, or the number and associated bounds of the elements used to describe the problem. Population size, N_p, is directly related to the number of elements n by $N_p = 10n$. The parameters K and F can theoretically take any value between 0 and 1. Traditionally, the level of recombination, K, can take values 0 (which by definition means mutation only, resulting in a random walk), 0.5 or 1 (Price, 1999), although in this case K is set at 0.99 and not exactly at 1, reducing the probability of stagnation (Lampinen & Zelinka, 2000). Our tests have shown optimal convergence at $K = 0.99$. The mutation function, F, is used both to disrupt good members of the population and to introduce new information to poor members. For optimal searching, a balance of these two effects is required: small values of F result in small amounts of disruption and premature convergence, whereas large values interrupt the natural selection process, and so median values are favoured. These three parameters are all allocated values at the start of the calculation, whereas either G_{max} can be defined at the start of the calculation or the process can be repeated until convergence has been achieved, *i.e.* until the mean R_{wp} of the population is the same as the R_{wp} of the best member (Figs. 1–3).

The best results from a number of initial DE calculations can then be used to seed a 'Mini DE' to ensure that the true minimum has been located. A 'Mini DE' calculation is performed like a conventional DE search but includes the best solution from each initial calculation in an otherwise randomly initialized population. The incorporation of 'promising' solutions in the population encourages rapid convergence on the solution minima, while the random population retains the necessary diversity to enable the search to proceed effectively.

3. Experimental

3.1. Materials

Samples of compounds (I)–(III) were purchased from Aldrich and used directly as received. Both (I) and (II) were obtained as fine white powders, whereas (III) was a fine orange powder.

3.2. Data collection

For X-ray powder diffraction data collection, all three samples were ground and then mounted in a disc between two layers of transparent tape. Data were collected for (I)–(III) in disc geometry at room temperature using a BrukerAXS D5000 powder diffractometer with Ge-monochromated Cu $K\alpha_1$ radiation ($\lambda = 1.5405$ Å) and a position-sensitive detector covering 8° in 2θ. The data were recorded in the range $4^\circ \leq 2\theta \leq 55^\circ$ in 0.01925° steps over a total of 1 h. In the case of (II), a second data set was recorded in capillary geometry with the sample loaded into a 0.5 mm capillary to a depth of approximately 3 cm. Data were collected at room temperature on a BrukerAXS D5005 powder diffractometer with Gobel mirrors and a position-sensitive detector with radial slits covering 8° in 2θ. Cu $K\alpha_{1,2}$ radiation ($\lambda = 1.5418$ Å) was used, and the beam size was 0.6 mm × 1 cm. The data were collected over the range $10^\circ \leq 2\theta \leq 50^\circ$ in 0.01943° steps for a total of 6 h.

4. Structure solution and refinement

The powder diffraction patterns collected for compounds (I)–(III) were indexed using the *CRYSFIRE* package (Shirley, 2000) on the basis of the first 20 observable reflections, and a space group was assigned to each material by consideration of systematic absences. For each structure, the profile parameters were refined by the whole-profile-fitting LeBail method in the program *GSAS* (Larson & Von Dreele, 1987) to improve the fit of the lattice and profile parameters. Structure solution was then performed using the differential evolution method as previously detailed in §2 and implemented in the program *POSSUM* (Seaton & Tremayne, 2002*b*). The parameters used in structure solution and refinement of (I)–(III) are summarized in Table 1,[1] and details of the solution process for each structure are given below.

4.1. 2-Toluenesulfonamide

The structural model of (I) used in the DE calculation comprised the complete molecule constructed using standard bond lengths and angles, excluding the amino and methyl H atoms. Structure solution required variation of the translation and orientation of the structural model around three mutually perpendicular axes within the unit cell, with the benzene ring treated as a rigid body and the sulfonamide group allowed to rotate freely as shown in Scheme 1. Thus each member of the population consisted of seven elements, with the initial position, orientation and intramolecular geometry of the structural model chosen arbitrarily and the upper and lower bounds on the elements set to [0, 1], [0, 360°] and [0, 360°], respectively. The population size was fixed at 70 members, and the maximum number of generations for each DE calculation set to 200.

Four initial DE calculations were carried out, with $K = 0.99$ and F having values 0.1, 0.2, 0.3 and 0.4; the results of these calculations were then used as the seed for a Mini DE (Fig. 1). This was run with parameters $K = 0.99$ and $F = 0.3$ and returned a solution significantly better than that obtained from the initial DE results and clearly distinguishable from the average random structures generated in the DE calculation (Table 1). This solution was then successfully refined as described in §4.4.

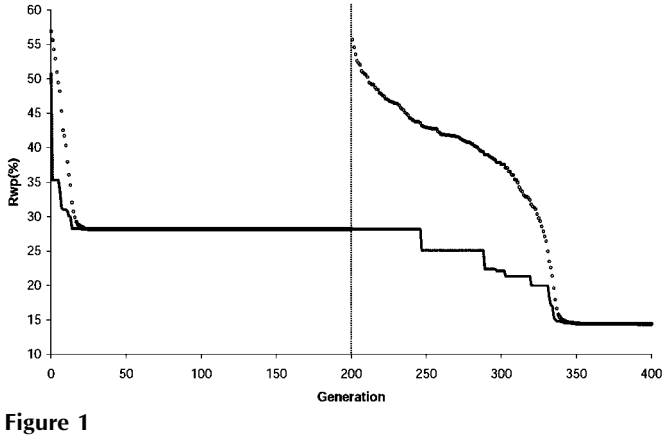

Figure 1
Differential evolution progress plot for the structure solution of (I), showing the best R_{wp} (line) and mean R_{wp} (open circles) for the initial DE calculation (generation 0–200) and the Mini DE calculation (generation 200–400).

[1] Supplementary data for this paper are available from the IUCr electronic archives (Reference: BM0052). Services for accessing these data are described at the back of the journal.

4.2. 3-Nitrobenzenesulfonamide

The structural model of (II) used for structure solution also comprised the complete molecule, constructed using standard bond lengths and angles but with the amino H atoms excluded. Movement of the structural model around the unit cell was carried out as before, with an additional element required to describe conformational flexibility of the nitro group relative to the benzene ring (Scheme 1). Thus each member of the population consisted of eight elements, and the population size was set at 80 members. The upper and lower bounds on these elements and the maximum number of generations were defined as for (I).

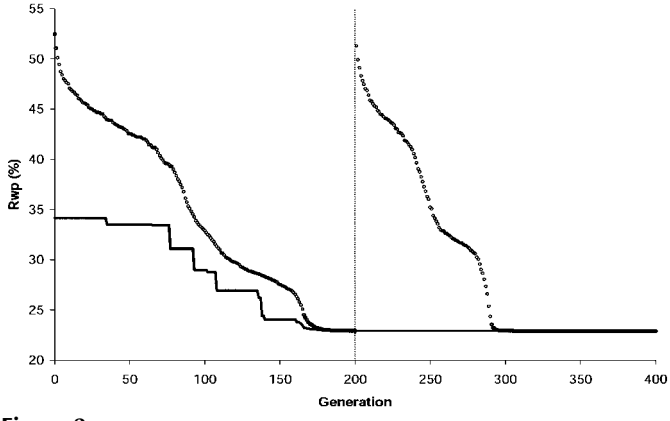

Figure 2
Differential evolution progress plot for the structure solution of (II). R_{wp} for initial and Mini DE calculation as depicted in Fig. 1.

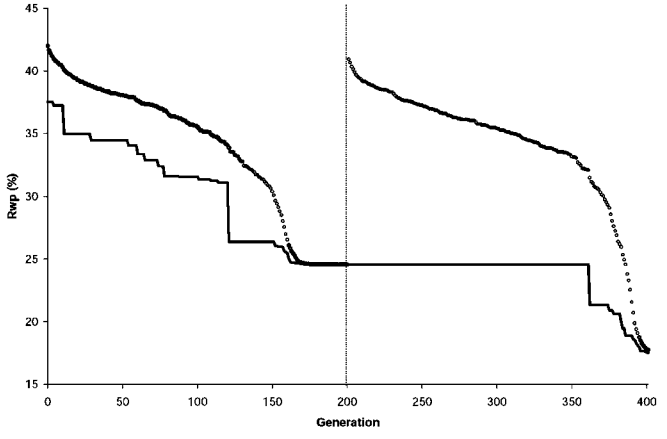

Figure 3
Differential evolution progress plot for the structure solution of (III). R_{wp} for initial and Mini DE calculation as depicted in Fig. 1.

Table 1
Initial lattice parameters, differential evolution structure solution parameters, final refined parameters, and agreement factors for (I)–(III).

For compound (II), the agreement factors (R_{wp} and χ^2) are for disc data (structure solution) and for capillary data (refinement).

Compound	(I)	(II)	(III)
Crystal data			
Chemical formula	$C_7H_9NO_2S$	$C_6H_6N_2O_4S$	$C_6H_6N_2O_4S$
Chemical formula weight	171.22	202.20	202.20
Cell setting, space group	Tetragonal, $I4_1/a$	Monoclinic, $P2_1$	Monoclinic, $P2_1/n$
Z	16	2	4
D_x (g cm^{-3})	1.423	1.638	1.618
μ (mm^{-1})	3.197	3.452	3.410
$F(000)$	1440	208	416
Radiation type	Cu $K\alpha_1$	Cu $K\alpha_{1,2}$	Cu $K\alpha_1$
Temperature (K)	273 (2)	273 (2)	273 (2)
Indexing			
Initial a (Å)	18.954	7.714	8.843
Initial b (Å)	= a	8.054	13.493
Initial c (Å)	9.201	7.036	7.076
Initial β (°)		110.27	100.48
Structure solution			
LeBail R_{wp}	9.00	5.28	5.40
LeBail χ^2	2.70	15.34	2.66
Elements	7	8	8
K	0.99	0.99	0.99
Best F	0.1	0.3	0.4
Average R_{wp}	57.00	51.00	40.00
Best R_{wp}	28.18	22.92	24.54
Mini DE − R_{wp}	14.40	22.89	17.51
Min Δx (Å)	0.10	0.02	0.18
Max Δx (Å)	0.49	0.44	0.55
Mean Δx (Å)	0.28	0.17	0.34
Refinement			
R_{wp}	9.75	6.25	7.19
R_p	7.69	4.66	5.29
R_F^2	10.78	6.66	16.46
χ^2	3.16	21.42	4.79
Preferred orientation fraction [and direction]		1.13 [101]	
No. of parameters	56	65	64
No. of restraints	39	47	47
Final a (Å)	18.7407 (8)	7.7169 (2)	8.8424 (3)
Final b (Å)	= a	8.0514 (2)	13.4933 (4)
Final c (Å)	9.1004 (4)	7.0334 (2)	7.0732 (2)
Final β (°)		110.274 (1)	100.466 (2)
V (Å^3)	3196.2 (3)	409.93 (2)	829.89 (2)

Ten initial DE calculations were carried out with $K = 0.99$ and F taking the values 0.1, 0.2, . . . , 1. The best five results were then used to seed the Mini DE (Fig. 2), run with $K = 0.99$ and $F = 0.3$. In this case, the solution returned by the Mini DE showed little improvement over the structure generated by the best initial structure solution calculation. Both these solutions give significantly lower R_{wp} values than those obtained from the average random structures generated in the DE calculation (Table 1).

However, after several cycles of refinement of this structure it was clear that the molecule had become significantly distorted. One possible explanation for this distortion is the presence of preferred orientation in the sample. Preferred orientation arises when crystallites have a tendency to align along a certain direction resulting in non-random distribution of crystallite orientations in the sample, affecting the relative intensities of given peaks. This is often most severe when the morphology is strongly anisotropic (*e.g.* flat plates or long needles), and the effects were minimized in this case by packing the sample in a capillary, hence reducing the effect of the plate-like crystallites. Comparison of the capillary data set with the initial data recorded using a flat disc confirmed the presence of a preferred orientation, and hence the capillary data was used for refinement, although variation of a preferred orientation parameter was still required along the [101] direction.

4.3. 4-Nitrobenzenesulfonamide

Structure solution of (III) was carried out in a similar way to that for (II), differing only in the position of the nitro group in the structural model (Scheme 1), *i.e.* requiring consideration of eight elements and a population size of 80. The initial DE calculations employed similar parameters to those used above, except that F was limited to the range 0.2–0.6, and the results of these five runs were used to seed the Mini DE (Fig. 3). This was run again with $K = 0.99$ and $F = 0.3$, and returned a solution significantly better than that obtained from the initial DE results and clearly distinguishable from the average random structures generated in the DE calculation (Table 1). This structure was successfully refined using the disc data set as described below.

4.4. Rietveld refinement

All three structures were refined using the *GSAS* program package (Larson & Von Dreele, 1987). The positions of all atoms were refined subject to restraints (weighting factor of 0.001 for bond distances and 0.005 for geminal non-bonded distances) on standard geometry. The amino H atoms in each structure were placed in positions calculated from the coordinates of the hydrogen-bond donors and acceptors, and the methyl H atoms in (I) modelled in at the usual geometry and conformation. For the non-H atoms, isotropic atomic displacement parameters were refined but constrained according to atom type or environment (*i.e.* S, amino or nitro N, amide or nitro O, aromatic or methyl C). The final Rietveld plots for (I)–(III) are shown in Figs. 4, 5 and 6, and the final agreement factors from refinement are given in Table 1. A comparison between the molecular positions found in the DE solutions and the refined crystal structures of (I)–(III) shows how effectively the DE method locates the solution corresponding to a global minimum in R_{wp} in each case. The minimum, maximum and mean distances (Δx) between pairs of corresponding non-H atoms in these structures are given in Table 1.

5. Description of the structures

5.1. Molecular conformations

The molecular dimensions of structures (I)–(III) are similar to those obtained from powder refinements of other sulfonamides with intramolecular bond lengths and angles showing

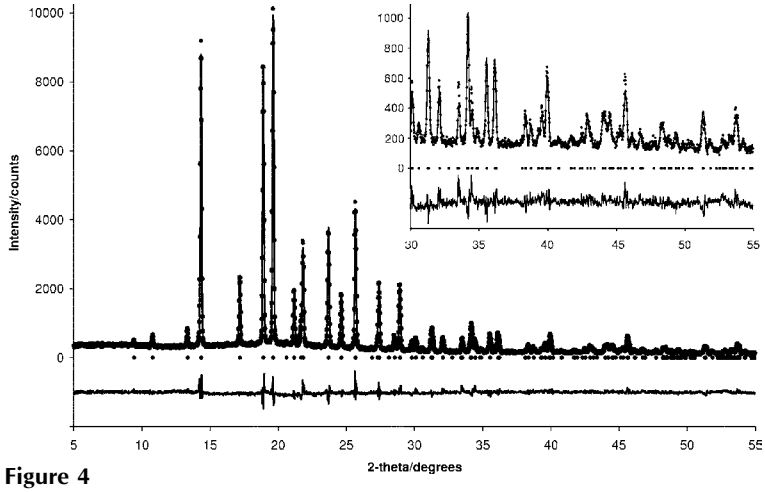

Figure 4
Final observed (black circles), calculated (solid line) and difference (below) X-ray powder diffraction profile for the final Rietveld refinement of (I). Reflection positions are also marked.

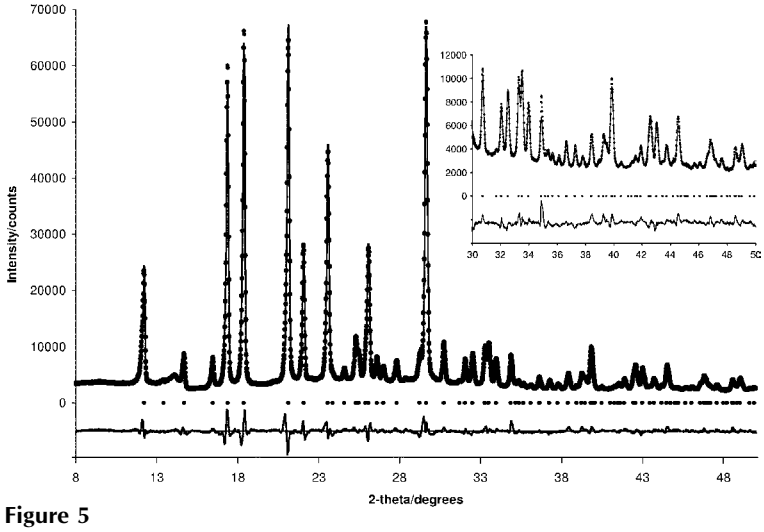

Figure 5
X-ray powder diffraction profile for the final Rietveld refinement of (II) (as in Fig. 4).

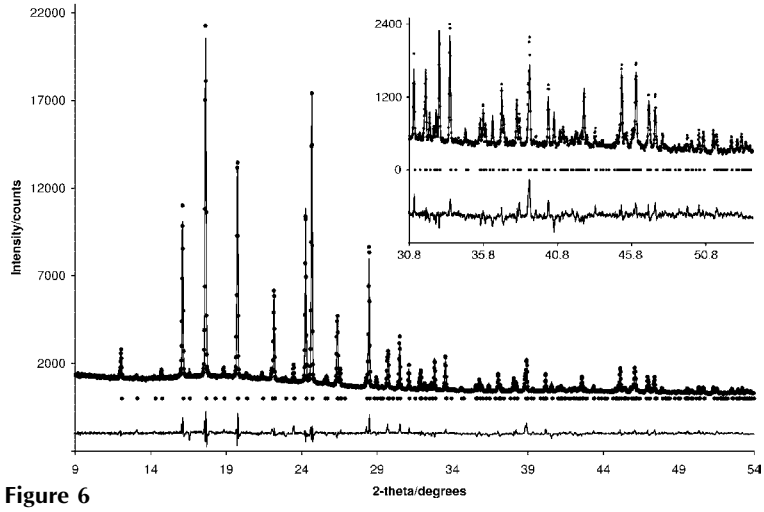

Figure 6
X-ray powder diffraction profile for the final Rietveld refinement of (III) (as in Fig. 4).

no unusual features (Figs. 7*a*–7*c*). The conformations of the sulfonamide and nitro groups [in (II) and (III)], which were allowed to move freely in both solution and refinement, also show values that are typically found in similar systems. As expected, the nitro groups in both (II) and (III) lie approximately in the plane of the aryl ring [C2—C3—N3—O31 = 20°, C2—C3—N3—O32 = 168° in (II); C3—C4—N4—O41 = −164°, C3—C4—N4—O42 = −3° in (III)]. However, the conformation of the sulfonamide group differs for each structure: compound (I) displays the most common sulfonamide conformation with an S—O bond (in this case involving O11) approximately parallel to the aryl ring (C2—C1—S1—O11 = −168°, C2—C1—S1—O12 = −36°, C2—C1—S1—N1 = 78°), whereas in (III) it is the amide N1 that lies in the plane of the ring (C2—C1—S1—N1 = 176°, C2—C1—S1—O11 = −75°, C2—C1—S1—O12 = 41°); compound (II) illustrates another characteristic conformation in which the C—S—N plane is approximately normal to that of the aryl ring (C2—C1—S1—N1 = −87°, C2—C1—S1—O11 = 154°, C2—C1—S1—O12 = 31°).

5.2. Supramolecular aggregation

5.2.1. 2-Toluenesulfonamide. In compound (I), the supramolecular aggregation is determined solely by two hard hydrogen bonds (Table 2): there are no intermolecular C—H···O hydrogen bonds and no aromatic $\pi\cdots\pi$ stacking interactions. These hard hydrogen bonds link the molecules into a continuous three-dimensional framework, which can be analysed in terms of two primary motifs (generated by each hydrogen bond in turn) that combine to form a secondary hydrogen-bond network.

Atom N1 at (x, y, z) acts as hydrogen-bond donor, *via* H11, to O11 at ($-\frac{1}{4}+y$, $\frac{3}{4}-x$, $-\frac{1}{4}+z$), while N1 at ($-\frac{1}{4}+y$, $\frac{3}{4}-x$, $-\frac{1}{4}+z$) acts as donor to O11 at ($\frac{1}{2}-x$, $1-y$, $-\frac{1}{2}+z$) and so on; propagation of this hydrogen bond produces a $C(4)$ spiral chain running parallel to the [001] direction and generated by the 4_1 screw axis along ($\frac{1}{4}$, $\frac{1}{2}$, z) (Fig. 8). Four spiral chains run through each unit cell, with those along [$\frac{1}{4}$, 0, $-z$] and [$\frac{3}{4}$, $\frac{1}{2}$, $-z$] having the opposite hand to those along ($\frac{1}{4}$, $\frac{1}{2}$, z) and ($\frac{3}{4}$, 0, z). The amino N1 also acts as hydrogen-bond donor, this time *via* H12, to O12 at ($\frac{5}{4}-y$, $\frac{1}{4}+x$, $\frac{5}{4}-z$), and propagation of this hydrogen bond produces an $R_4^4(16)$ ring lying around the $\bar{4}$ axis along ($\frac{1}{2}$, $\frac{3}{4}$, z) with centroid ($\frac{1}{2}$, $\frac{3}{4}$, $\frac{5}{8}$) (Fig. 9). The four molecules within this ring are components of four different $C(4)$ spiral chains, those along ($\frac{1}{4}$, 0, $-z$), ($\frac{1}{4}$, $\frac{1}{2}$, z), ($\frac{3}{4}$, $\frac{1}{2}$, $-z$) and ($\frac{3}{4}$, 1, z). The linking of the $C(4)$ chains can alternatively be considered in terms of the combined effect of the two hydrogen bonds forming a secondary motif: the molecules at (x, y, z) and ($1-x$, $-y$, $1-z$) are both linked to those at ($-\frac{1}{4}+y$, $\frac{3}{4}-x$,

Table 2
Intermolecular hydrogen-bond parameters (Å,°) for (I)–(III).

D—H···A	H···A	D···A	D—H···A	Motif	Direction
Compound (I)					
N1—H11···O11^{i}	1.84	2.91 (2)	178	$C(4)$	[001]
N1—H12···O12^{ii}	2.01	3.04 (2)	178	$R_4^4(16)$	–
Compound (II)					
N1—H11···O11^{iii}	2.06	3.07 (2)	177	$C(4)$	[010]
N1—H12···O12^{iv}	2.03	3.04 (2)	176	$C(4)$	[010]
C4—H4···O12^{v}	2.41	3.30 (2)	136	$C(7)$	[101]
Compound (III)					
N1—H11···O11^{vi}	2.16	3.15 (1)	179	$C(4)$	[101]
N1—H12···O41^{vii}	2.14	3.15 (1)	179	$C(9)$	[10$\bar{1}$]
C2—H2···O41^{viii}	2.32	3.25 (2)	141	$C(6)$	[001]
C5—H5···O12^{ix}	2.39	3.27 (2)	135	$C(6)$	[001]

Symmetry codes: (i) $-\frac{1}{4}+y, \frac{3}{4}-x, -\frac{1}{4}+z$; (ii) $\frac{5}{4}-y, \frac{1}{4}+x, \frac{5}{4}-z$; (iii) $2-x, -\frac{1}{2}+y, 1-z$; (iv) $2-x, \frac{1}{2}+y, 1-z$; (v) $-1+x, y, -1+z$; (vi) $\frac{1}{2}+x, \frac{3}{2}-y, \frac{1}{2}+z$; (vii) $\frac{1}{2}+x, \frac{3}{2}-y, -\frac{1}{2}+z$; (viii) $x, y, -1+z$; (ix) $x, y, 1+z$.

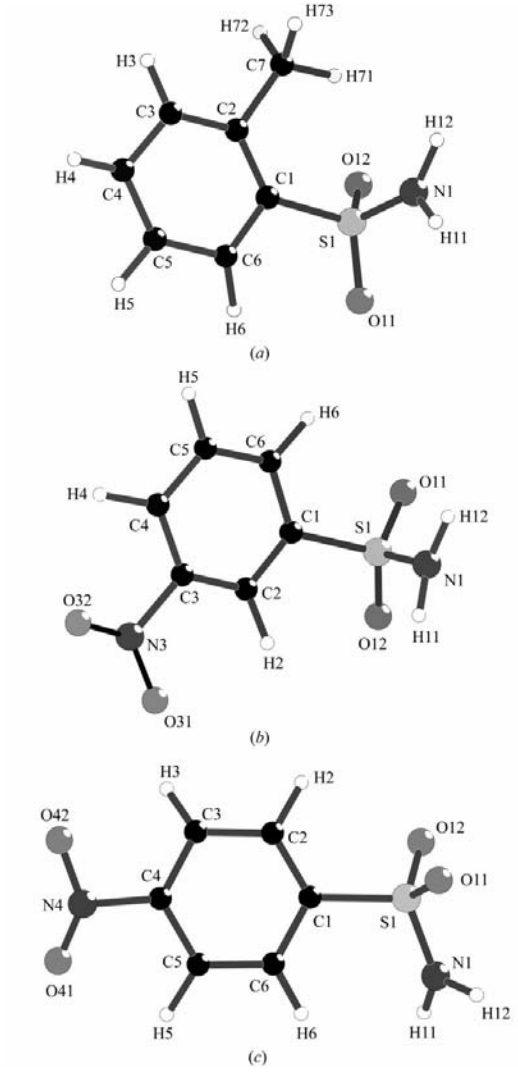

Figure 7
The refined molecular structures of (I)–(III) [(*a*)–(*c*), respectively], showing the conformation of each molecule and the atom-labelling scheme used in each case.

$-\frac{1}{4}+z$) and ($\frac{5}{4}-y, \frac{1}{4}+x, \frac{5}{4}-z$) to give a centrosymmetric $R_4^4(12)$ ring centred at ($\frac{1}{2}, \frac{1}{2}, \frac{1}{2}$) (Fig. 9), in which the four components lie in different $C(4)$ chains.

5.2.2. 3-Nitrobenzenesulfonamide. In compound (II), there are two hard hydrogen bonds of type N—H···O═S and a soft hydrogen bond of type C—H···O═S (Table 2): the nitro group is not involved in any hydrogen bonding.

The two N—H···O═S hydrogen bonds combine to form a molecular ladder or ribbon. The amino N1 at (x, y, z) acts as donor, *via* H11 and H12, respectively, to O11 at ($2-x, -\frac{1}{2}+y,$

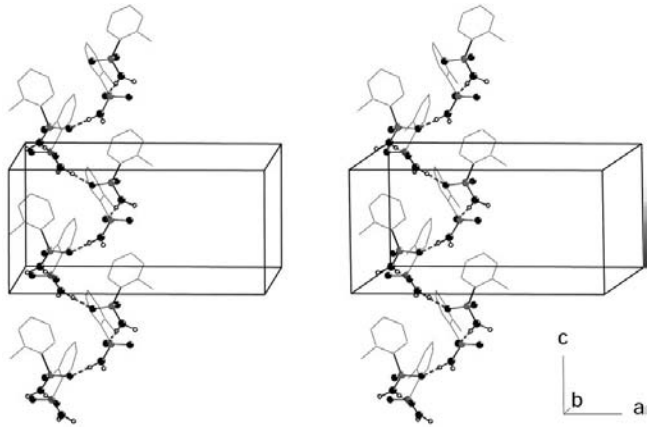

Figure 8
Stereoview of part of the crystal structure of (I), showing the $C(4)$ spiral chain along ($\frac{1}{4}, \frac{1}{2}, z$). S atoms are shown as light grey spheres, O as medium grey, N as black, C as dots and H as open circles; thick dashed lines represent N—H···O═S hydrogen bonds. Only H atoms involved in hydrogen bonding are shown.

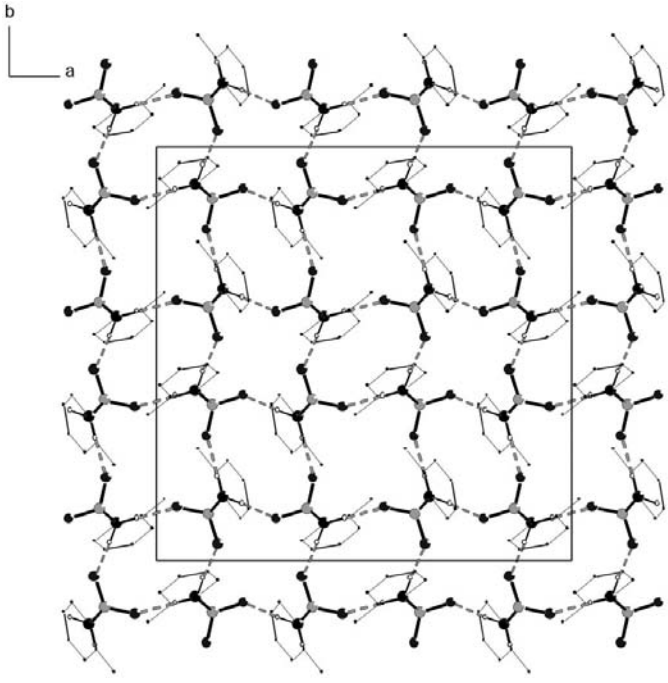

Figure 9
Projection on the (001) plane of the crystal structure of (I) showing the $R_4^4(16)$ and $R_4^4(12)$ rings linking the $C(4)$ chains into a single three-dimensional framework. Atoms and bonds are depicted as in Fig. 8.

$1 - z$) and to O12 at ($2 - x, \frac{1}{2} + y, 1 - z$), so forming a pair of $C_2^2(6)$ chains running parallel to the [010] direction and generated by the 2_1 screw axis along ($1, y, \frac{1}{2}$). These chains act as the uprights of the molecular ladder, while the N—S bonds act as the rungs, with $R_2^2(8)$ rings between these rungs (Fig. 10). While the $R_2^2(8)$ ring motif is typical of sulfonamide aggregation, the paired $C_2^2(6)$ chain motif is unusual, although this motif can be deconstructed into a pair of criss-cross $C(4)$ chains comprising the atom sequences H11—N1—S1—O11 and H12—N1—S1—O12.

There are no aromatic $\pi\cdots\pi$ stacking interactions in compound (II), but there is a single C—H$\cdots$O═S hydrogen bond that links the [010] ladders into a ($10\bar{1}$) sheet. Atom *C*4 at (x, y, z) is a component of the ladder along ($1, y, \frac{1}{2}$) and it acts as hydrogen-bond donor to sulfonamide O12 at ($-1 + x, y, -1 + z$), which is a component of the ladder along ($0, y, -\frac{1}{2}$): similarly, *C*4 at ($2 - x, \frac{1}{2} + y, 1 - z$), which is also a component of the ($1, y, \frac{1}{2}$) ladder, acts as donor to O12 at ($3 - x, \frac{1}{2} + y, 2 - z$), which lies in the ladder along ($2, y, 1.5$). The C—H$\cdots$O hydrogen bonds thus generate a pair of antiparallel $C(7)$ chains along [101] (Fig. 11), and the combination of these chains with the [010] ladders generates the ($10\bar{1}$) bilayer.

5.2.3. 4-Nitrobenzenesulfonamide. The supramolecular structure of compound (III) is dominated by two N—H$\cdots$O hydrogen bonds (Table 2), one each of types N—H$\cdots$O═S and N—H$\cdots$O(nitro), in contrast to the hydrogen-bonding behaviour of compound (II), in which there is no participation of the nitro group in either the hard or the soft hydrogen bonds. These link the molecules into square (4, 4) nets (Batten & Robson, 1998) that can be analysed in terms of two one-dimensional chain-forming motifs.

The amino N1 at (x, y, z) acts as hydrogen-bond donor, *via* H11, to sulfonamide O11 at ($\frac{1}{2} + x, \frac{3}{2} - y, \frac{1}{2} + z$), while N1 at ($\frac{1}{2} + x, \frac{3}{2} - y, \frac{1}{2} + z$) in turn acts as donor to O11 at ($1 + x, y, 1 + z$). This hydrogen bond produces the $C(4)$ chain motif so characteristic of sulfonamides: the chain runs parallel to the [101] direction and is generated by the *n*-glide plane at $y = \frac{3}{4}$. N1 at (x, y, z) also acts as donor, this time *via* H12, to nitro O41 at ($\frac{1}{2} + x, \frac{3}{2} - y, -\frac{1}{2} + z$), and propagation of this hydrogen

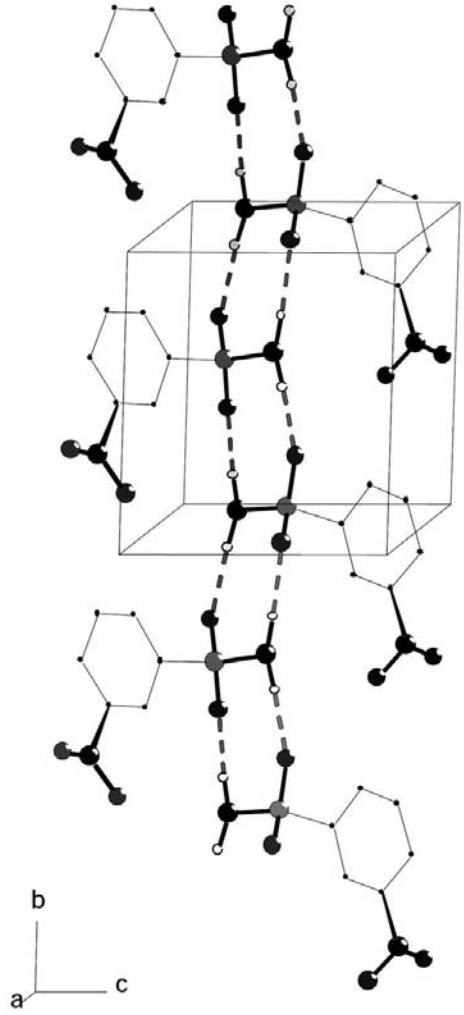

Figure 10
Part of the crystal structure of (II) showing the molecular ladder along [010] formed by the hard hydrogen bonds. Atoms and bonds are depicted as in Fig. 8.

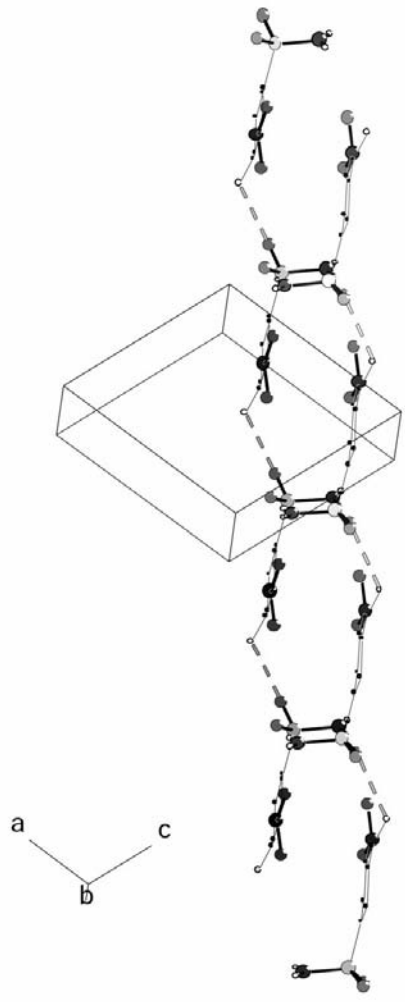

Figure 11
Part of the crystal structure of (II) showing the $C(7)$ chain along [101] formed by the soft hydrogen bonds. Atoms and bonds are depicted as in Fig. 8.

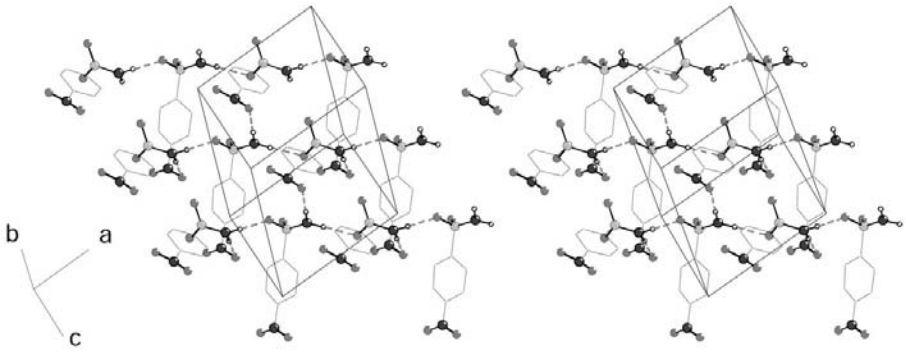

Figure 12
Stereoview of part of the crystal structure of (III) showing the formation of a (010) sheet of $R_4^4(24)$ rings generated by the hard hydrogen bonds. Atoms and bonds are depicted as in Fig. 8.

bond produces a $C(9)$ chain along the $[10\bar{1}]$ direction, generated by the same glide plane as the [101] chain. The combination of the two chain motifs generates a (010) sheet in the form of a (4, 4) net built from a single type of $R_4^4(24)$ ring (Fig. 12).

The sheet formation is reinforced by two C—H···O hydrogen bonds, one each of the types C—H···O═S and C—H···O(nitro), with aryl C as the donor in each case (Table 2). Atoms C2 and C5 in the molecule at (x, y, z) act as hydrogen-bond donors to nitro O41 at (x, y, $-1+z$) and sulfonamide O12 at (x, y, $1+z$), respectively. Thus, although both sulfonamide O atoms act as hydrogen-bond acceptors, one each from N and C, the nitro O41 atom acts as a double acceptor (again from N and C), while O42 is not involved in the hydrogen bonding. The two soft hydrogen bonds together generate by translation a $C(6)C(6)[R_2^2(10)]$ chain of rings (Bernstein *et al.*, 1995) running parallel to the [001] direction (Fig. 13).

There are two (010) sheets passing through each unit cell, one in the domain $0.42 < y < 1.08$ and the other in the domain $-0.08 < y < 0.58$, with each sheet linked to two neighbouring sheets by weak aromatic $\pi\cdots\pi$ stacking interactions. The aryl rings of the molecules at (x, y, z) and ($1-x$, $2-y$, $2-z$) are parallel with an interplanar spacing of ~3.59 Å and a centroid offset of ~1.76 Å (Fig. 14): these two molecules lie in the domains $0.42 < y < 1.08$ and $0.92 < y < 1.58$, respectively. There is a similar stacking interaction between the aryl ring in the molecule at ($\frac{1}{2}+x$, $\frac{3}{2}-y$, $\frac{1}{2}+z$), also in the domain $0.42 < y < 1.08$, and that in the molecule at ($\frac{3}{2}-x$, $-\frac{1}{2}+y$, $\frac{5}{2}-z$), which lies in the domain $-0.08 < y < 0.58$. Hence, each (010) sheet is linked to the two adjacent sheets.

5.2.4. Other sulfonamides and sulfonylhydrazines. The supramolecular structure reported here for the simple sulfonamide (I), (where we use 'simple' to denote the absence of any other potential hydrogen-bonding substituents in the aryl ring), may usefully be compared with those of other simple sulfonamides and sulfonylhydrazines, also deduced from X-ray powder diffraction data. Table 3 compares the N—H···O hydrogen bonds and gives details of the resulting unitary and secondary hydrogen-bond networks, which are present in a number of simple sulfonamides and sulfonylhydrazines.

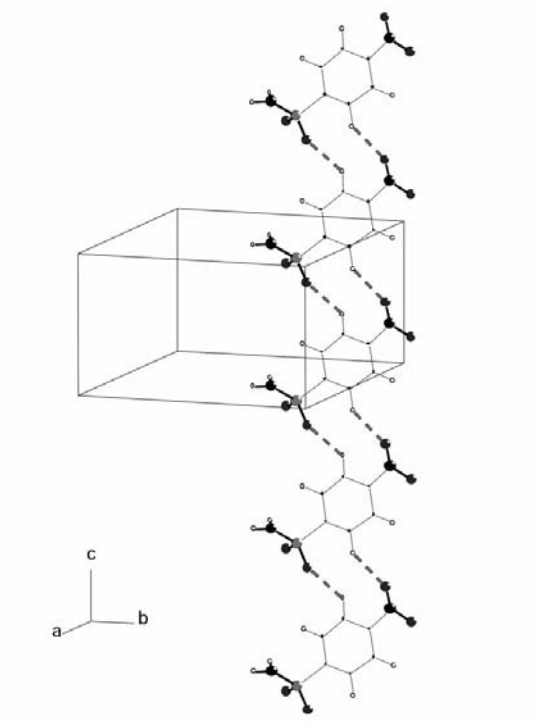

Figure 13
Part of the crystal structure of (III) showing the formation of a [001] chain of rings generated by the soft hydrogen bonds. Atoms and bonds are depicted as in Fig. 8, except that all H atoms are shown.

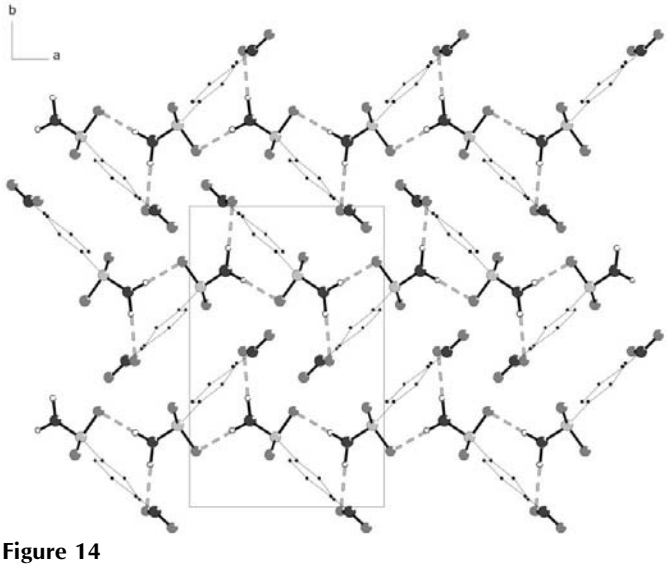

Figure 14
Part of the crystal structure of (III) showing three hydrogen-bonded sheets linked by aromatic stacking interactions (the $\pi\cdots\pi$ interactions are not shown). Atoms and bonds are depicted as in Fig. 8.

Table 3
Hydrogen-bond distances (Å), motifs and networks for selected simple sulfonamides and sulfonylhydrazines.

Atom labelling in hydrazines follows that in Lightfoot *et al.* (1993):

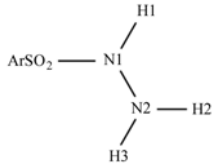

Compound	D—H···A	D···A	Motif	[Direction] or (plane)	Secondary network and (plane)
o-$CH_3C_6H_4SO_2NH_2$	N1—H11···O11^{i}	2.91 (2)	$C(4)$	[001]	
	N1—H12···O12^{ii}	3.04 (2)	$R_4^4(16)$	–	$R_4^4(12)$
p-$CH_3C_6H_4SO_2NH_2$†	N—H1···O1^{iii}	2.87 (1)	$C(4)$	[101]	
	N—H2···O2^{iv}	2.99 (1)	$C(4)$	[$\bar{1}$01]	$R_4^4(14)$ (010)
$(Me_2CH)_3C_6H_4SO_2NH_2$‡	N—H1···O2^{v}	2.77 (1)	$C(4)$	[010]	
	N—H2···O1^{vi}	2.92 (1)	$R_2^2(8)$	(100)	$R_6^6(20)$ (100)
$C_6H_5SO_2NHNH_2$†	N2—H2···O1	2.91 (2)	$S(5)$	–	
	N1—H1···O1^{vii}	3.14 (1)	$C(4)$	[010]	$R_4^4(14)$ (100)
	N2—H3···O2^{viii}	3.15 (1)	$C(5)$	[001]	$R_4^4(18)$ (100)
p-$CH_3C_6H_4SO_2NHNH_2$†	N2—H2···O1^{ix}	3.13 (1)	$C(5)$	[010]	
	N1—H1···O2^{x}	3.13 (1)	$C(4)$	[010]	$R_3^2(9)$ (100)
	N2—H3···O1^{xi}	2.87 (1)	$C(5)$	[010]	$R_3^3(11)$ (100)

Symmetry codes: (i) $-\frac{1}{4}+y, \frac{3}{4}-x, -\frac{1}{4}+z$; (ii) $\frac{5}{4}-y, \frac{1}{4}+x, \frac{5}{4}-z$; (iii) $-\frac{1}{2}+x, \frac{1}{2}-y, -\frac{1}{2}+z$; (iv) $-\frac{1}{2}+x, \frac{1}{2}-y, \frac{1}{2}+z$; (v) $-x, \frac{1}{2}+y, \frac{3}{2}-z$; (vi) $-x, 1-y, 1-z$; (vii) $2-x, -\frac{1}{2}+y, \frac{3}{2}-z$; (viii) $x, \frac{1}{2}-y, -\frac{1}{2}+z$; (ix) $x, 1+y, z$; (x) $\frac{3}{2}-x, \frac{1}{2}+y, \frac{1}{2}-z$; (xi) $\frac{3}{2}-x, \frac{1}{2}+y, \frac{3}{2}-z$. † Lightfoot *et al.* (1993). ‡ Tremayne *et al.* (1999).

The hydrogen-bonded supramolecular structure of $(Me_2CH)_3C_6H_2SO_2NH_2$ has recently been described and analysed in detail (Tremayne *et al.*, 1999), and here we comment further on three examples (Table 3) originally reported some years ago (Lightfoot *et al.*, 1993). In that original study, no H atoms were located or included in the structural models, and hydrogen-bonding schemes were deduced from consideration of non-bonded intra- and intermolecular contacts involving potential hydrogen-bond donors and acceptors. We have now taken the coordinates of the non-H atoms from that study and, using simple model-building techniques, incorporated the H atoms at the most plausible sites, as judged by consideration both of intramolecular bond lengths and angles and of the intermolecular contacts. Supramolecular analysis of the resulting systems using *PLATON* (Spek, 2002) allows an analysis and description of the molecular aggregation and packing that is much more detailed than was possible originally (Lightfoot *et al.*, 1993).

In *p*-$CH_3C_6H_4SO_2NH_2$, which crystallizes in space group $P2_1/n$, the amino N acts as hydrogen-bond donor *via* H1 to O1 at $(-\frac{1}{2}+x, \frac{1}{2}-y, -\frac{1}{2}+z)$ and *via* H2 to $(-\frac{1}{2}+x, \frac{1}{2}-y, \frac{1}{2}+z)$, so giving a pair of $C(4)$ chains running parallel to the [101] and [10$\bar{1}$] directions, respectively. The combination of these chains generates a (010) sheet built from a single type of $R_4^4(14)$ ring (Fig. 15): two such sheets, related to one another by the centres of inversion run through each unit cell, generated by *n*-glide planes at $y = \frac{1}{4}$ and $y = \frac{3}{4}$. In each sheet there is a central polar layer comprising the sulfonamide units, with aromatic rings pendent from both faces: there are, however, no $\pi\cdots\pi$ stacking interactions between aromatic units in adjacent layers. The overall supramolecular architecture of *p*-$CH_3C_6H_4SO_2NH_2$ is thus rather similar to the sandwich structure of $(Me_2CH)_3C_6H_2SO_2NH_2$ (Tremayne *et al.*, 1999).

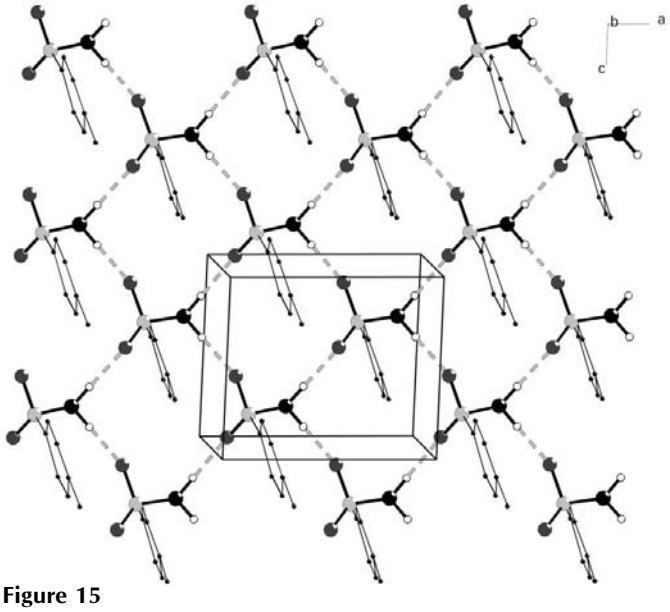

Figure 15
View of the crystal structure of *p*-toluenesulfonamide showing the $C(4)$ chains linked together to form a hydrogen-bonded sheet of $R_4^4(14)$ rings in the (010) plane. Atoms and bonds are depicted as in Fig. 8.

The sulfonylhydrazine $PhSO_2NHNH_2$, which crystallizes in $P2_1/c$, contains an intramolecular $S(5)$ motif, leaving two N—H bonds, one at each N, available for intermolecular aggregation (Table 3). N1 acts as hydrogen-bond donor to O1 at $(2-x, -\frac{1}{2}+y, \frac{3}{2}-z)$, so forming a $C(4)$ chain running parallel to [010] and generated by the 2_1 screw axis along $(1, y, \frac{3}{4})$: at the same time, N2 acts as hydrogen-bond donor to O2 at $(x, \frac{1}{2}-y, -\frac{1}{2}+z)$, forming a $C(5)$ chain running parallel to [001] and generated by the *c*-glide plane at $y = \frac{1}{4}$. Two chains of each type run through each unit cell and their combined effect is the formation of a (100) sheet built from $R_4^4(14)$ and $R_4^4(18)$ rings alternating in checkerboard fashion (Fig. 16). Once again, the individual sheet exhibits a sandwich structure with a polar core layer in between layers of aromatic groups; as in the structure of *p*-$CH_3C_6H_4SO_2NH_2$, there are no aromatic $\pi\cdots\pi$ stacking interactions between adjacent sheets.

The supramolecular structure of p-$CH_3C_6H_4SO_2NHNH_2$ (space group $P2_1/n$) again takes the form of sandwich-type sheets with a polar central layer, but the hydrogen bonding within each sheet is more complex than in the previous examples, since all of the N—H bonds are involved in intermolecular aggregation. Atoms N1 and N2 at (x, y, z) act as hydrogen-bond donors, respectively, to O2 at ($\frac{3}{2}-x$, $\frac{1}{2}+y$, $\frac{1}{2}-z$) and to O1 at ($\frac{3}{2}-x$, $\frac{1}{2}+y$, $\frac{3}{2}-z$), so forming $C(4)$ and $C(5)$ chains, both running parallel to [010] and generated by the 2_1 screw axes along ($\frac{3}{4}$, y, $\frac{1}{4}$) and ($\frac{3}{4}$, y, $\frac{3}{4}$). The combination of these two motifs is sufficient to generate a (100) sheet, but this sheet is reinforced by a third hydrogen bond. N2 at (x, y, z) acts as donor, *via* H2, to O1 at (x, $1+y$, z), so generating by translation a second $C(5)$ motif parallel to [010]. The combination of these three chain motifs generates a sheet containing two distinct ring motifs, of $R_3^2(9)$ and $R_3^3(11)$ types, arranged in strips parallel to [010] (Fig. 17).

6. Concluding comments

In an earlier report (Lightfoot *et al.*, 1993) of the structure determination of a number of arenesulfonamides and arenesulfonylhydrazines using conventional laboratory-quality X-ray powder diffraction data, we also described unsuccessful attempts at structure solution both for compound (I) and for $(Me_2CH)_3C_6H_2SO_2NH_2$, and we remarked that success in these cases might be achievable in the future with improved instrumental resolution (*e.g.* using synchrotron radiation) and/or by the application of improved structure solution software. In both these cases, successful structure solution required the development of a new generation of such software: the structure solution for $(Me_2CH)_3C_6H_2SO_2NH_2$ was achieved (Tremayne *et al.*, 1999) using the Monte Carlo method with a data set collected using synchrotron radiation, and the structure solution for (I) reported here has been achieved using diffraction data collected some ten years ago, but solved using a new direct-space method based on the DE algorithm. Although not previously reported, earlier attempts at the structure solution of both (II) and (III) had also been unsuccessful.

We have demonstrated that powder diffraction data alone can be used to elucidate the structures and rationalize the hydrogen-bonding networks of a set of compounds that form a systematic crystallographic study of intermolecular interactions. Over the years, we have used a range of structure solution techniques in this study, including traditional direct methods, the maximum entropy and likelihood method, and more recently, direct-space methods based on Monte Carlo and DE algorithms. However, it is clear that it is the development of these direct-space methods that has played a major role in the successful structure determination of the majority of these compounds.

In this paper, we have also demonstrated the application of a new global optimization technique to structure solution from powder diffraction data. The DE method offers the robust searching of minima, typical of evolutionary algorithms, while

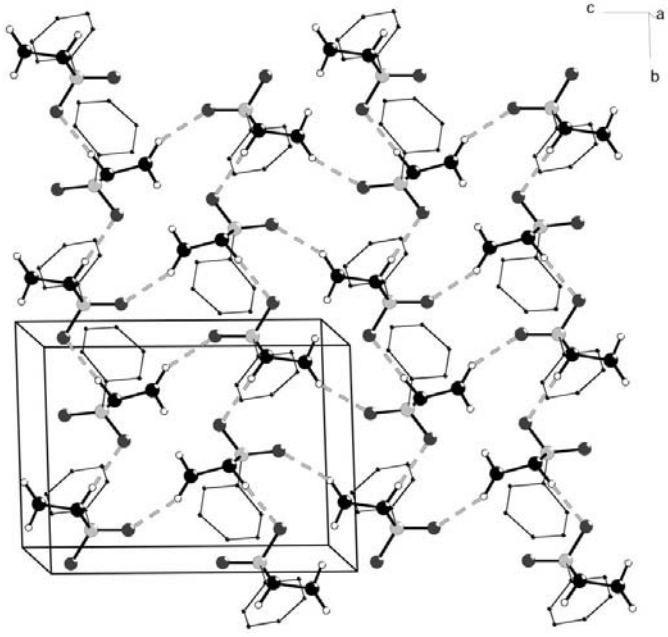

Figure 16
View of the crystal structure of benzenesulfonylhydrazine showing the formation of a (100) sheet of alternating $R_4^4(14)$ and $R_4^4(18)$ rings linking the $C(4)$ and $C(5)$ chains. Atoms and bonds are depicted as in Fig. 8, and intramolecular hydrogen bonds are not shown.

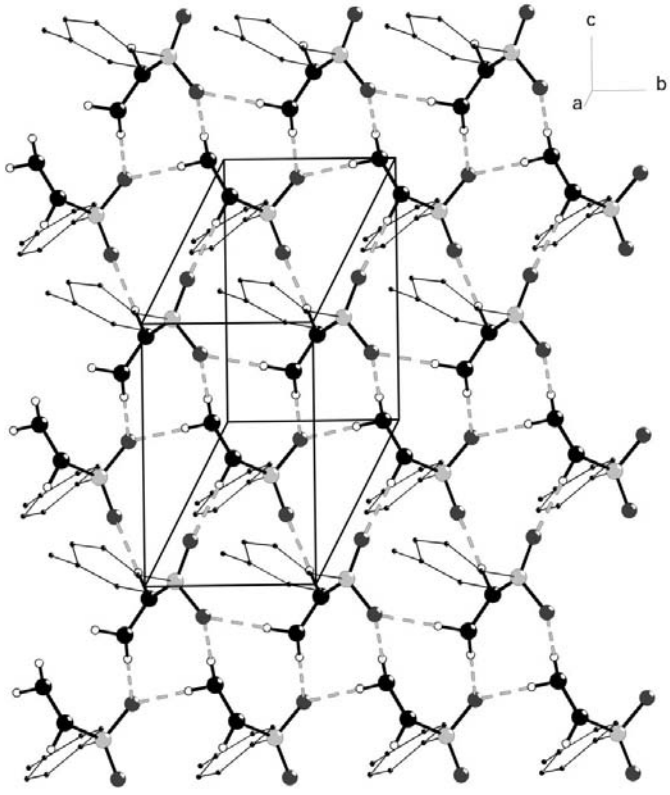

Figure 17
View of the crystal structure of p-toluenesulfonylhydrazine showing the combination of $C(4)$ and $C(5)$ chains forming a network of $R_3^2(9)$ and $R_3^3(11)$ rings in a slightly puckered continuous (100) sheet. Atoms and bonds are depicted as in Fig. 8.

being relatively simple to implement. We have found the DE method to be fast and reliable, with the power of the method being illustrated by the fact that the entire structure determination process for each structure presented here (including data collection and Rietveld refinement with all calculations performed on a desktop PC) was carried out 'in-house' within one working day. The DE calculation can be fully controlled with only four parameters, and the use of bounds associated with each structure element means that the incorporation of geometrical structure limits is straightforward. In the structure solution calculations of (I)–(III) (and in unpublished tests on known crystal structures), the DE control parameters were either defined according to the complexity of the structural problem (*i.e.* for $G_{\max}$ and N_p), or a number of calculations performed over a range of parameter values (*i.e.* for K and F). Our results show that the optimum structure solution is obtained from a limited range of K and F values, and they indicate that similar structural problems may be solved using a predefined set of control parameters without the need for multiple calculations.

MT is grateful to the Royal Society for the award of a University Research Fellowship: CCS thanks GlaxoSmith-Kline (UK) and the University of Birmingham for financial support.

References

Aakeröy, C. B., Beatty, A. M., Tremayne, M., Rowe, D. M. & Seaton, C. C. (2001). *Cryst. Growth Des.* **1**, 377–382.

Andreev, Y. G. & Bruce, P. G. (1998). *J. Chem. Soc. Dalton Trans.* pp. 4071–4080.

Andreev, Y. G., Lightfoot, P. & Bruce, P. G. (1997). *J. Appl. Cryst.* **30**, 294–305.

Batten, S. R. & Robson, R. (1998). *Angew. Chem. Int. Ed. Engl.* **37**, 1460–1494.

Bernstein, J., Davis, R. E., Shimoni, L. & Chang, N.-L. (1995). *Angew. Chem. Int. Ed. Engl.* **34**, 1555–1573.

Blaschette, A., Wieland, E., Schomburg, D. & Adelhelm, M. (1986). *Z. Anorg. Allg. Chem.* **533**, 7–17.

Braga, D., Grepioni, F., Biradha, K., Pedireddi, V. R. & Desiraju, G. R. (1995). *J. Am. Chem. Soc.* **117**, 3156–3166.

Brink, K. & Mattes, R. (1986). *Acta Cryst.* C**42**, 319–322.

Burgeni, A., Halla, F. & Kratky, O. (1929). *Z. Kristallogr.* **71**, 263–268.

Cannon, D., Glidewell, C., Low, J. N., Quesada, A. & Wardell, J. L. (2001). *Acta Cryst.* C**57**, 216–221.

Cheung, E. Y., McCabe, E. E., Harris, K. D. M., Johnston, R. L., Tedesco, E., Raja, K. M. P. & Balaram, P. (2002). *Angew. Chem. Int. Ed. Engl.* **41**, 494–496.

Chisholm, K. (1999). *New Ideas in Optimization*, edited by D. Corne, M. Dorigo & F. Glover, pp. 147–158. London: McGraw-Hill.

Cotton, F. A. & Stokely, P. F. (1970). *J. Am. Chem. Soc.* **92**, 294–302.

David, W. I. F., Shankland, K. & Shankland, N. (1998). *Chem. Commun.* pp. 931–932.

Ellena, J., Goeta, A. E., Howard, J. A. K., Wilson, C. C., Autino, J. C. & Punte, G. (1999). *Acta Cryst.* B**55**, 209–215.

Ferguson, G., Glidewell, C., Low, J. N., Skakle, J. M. S. & Wardell, J. L. (2001). *Acta Cryst.* C**57**, 315–316.

Harris, K. D. M., Johnston, R. L. & Kariuki, B. M. (1998). *Acta Cryst.* A**54**, 632–645.

Harris, K. D. M. & Tremayne, M. (1996). *Chem. Mater.* **8**, 2554–2570.

Harris, K. D. M., Tremayne, M. & Kariuki, B. M. (2001). *Angew. Chem. Int. Ed. Engl.* **40**, 1626–1651.

Harris, K. D. M., Tremayne, M., Lightfoot, P. & Bruce, P. G. (1994). *J. Am. Chem. Soc.* **116**, 3543–3547.

Kariuki, B. M., Serrano-Gonzalez, H., Johnston, R. L. & Harris, K. D. M. (1997). *Chem. Phys. Lett.* **280**, 189–195.

Klug, H. P. (1968). *Acta Cryst.* B**24**, 792–802.

Klug, H. P. (1970). *Acta Cryst.* B**26**, 1268–1275.

Lampinen, J. & Zelinka, I. (2000). *Proceedings of MENDEL 2000, Sixth International Mendel Conference on Soft Computing*, edited by P. Osmena, pp. 76–83. Brno, Czech Republic.

Larson, A. C. & Von Dreele, R. B. (1987). *GSAS. Generalized Structure Analysis System.* Report No. LAUR-86–748. Los Alamos National Laboratory, Los Alamos, New Mexico, USA.

Lightfoot, P., Tremayne, M., Glidewell, C., Harris, K. D. M. & Bruce, P. G. (1993). *J. Chem. Soc. Perkin Trans.* 2, pp. 1625–1630.

Nowell, H., Attfield, J. P., Cole, J. C., Cox, P. J., Shankland, K., Maginn, S. M. & Motherwell, W. D. S. (2002). *New J. Chem.* **26**, 469–472.

Pagola, S., Stephens, P. W., Bohle, D. S., Kosar, A. D. & Madsen, S. K. (2000). *Nature* (*London*), **404**, 307–310.

Ploug-Sørensen, G. & Andersen, E. K. (1986). *Acta Cryst.* C**42**, 1813–1815.

Price, K. V. (1999). *New Ideas in Optimization*, edited by D. Corne, M. Dorigo & F. Glover, pp. 77–158. London: McGraw-Hill.

Seaton, C. C. & Tremayne, M. (2002*a*). *Chem. Commun.* pp. 880–881.

Seaton, C. C. & Tremayne, M. (2002*b*). *POSSUM. Programs for Direct-Space Structure Solution from Powder Diffraction Data.* School of Chemical Sciences, University of Birmingham, UK.

Shankland, K., David, W. I. F., Csoka, T. & McBride, L. (1998). *Int. J. Pharm.* **165**, 117–126.

Shankland, N., David, W. I. F., Shankland, K., Kennedy, A. R., Frampton, C. S. & Florence, A. J. (2001). *Chem. Commun.* pp. 2204–2205.

Shirley, R. A. (2000). *CRYSFIRE. Suite of Programs for Indexing Powder Diffraction Patterns.* University of Surrey, UK.

Spek, A. L. (2002). *PLATON.* University of Utrecht, The Netherlands.

Storn, R. & Price, K. V. (1997). *J. Global Optim.* **11**, 341–359.

Tedesco, E., Harris, K. D. M., Johnston, R. L., Turner, G. W., Raja, K. M. P. & Balaram, P. (2001). *Chem. Commun.* pp. 1460–1461.

Tonogaki, M., Kawata, T., Ohba, S., Iwata, Y. & Shibuya, I. (1993). *Acta Cryst.* B**49**, 1031–1039.

Tremayne, M. & Glidewell, C. (2000). *Chem. Commun.* pp. 2425–2426.

Tremayne, M., Kariuki, B. M. & Harris, K. D. M. (1997). *Angew. Chem. Int. Ed. Engl.* **36**, 770–772.

Tremayne, M., MacLean, E. J., Tang, C. C. & Glidewell, C. (1999). *Acta Cryst.* B**55**, 1068–1074.

Vorontsova, L. G. (1966). *Zh. Strukt. Khim.* **7**, 280–283.